공학석사학위논문

Study on EGR estimation model by measuring temperatures and reduction of Diesel engine out emission through closed loop control based on the in-cylinder pressure with EGR model

온도 기반 EGR 예측 모델 개발과 EGR 예측 모델을 포함하는 연소압 기반 디젤 엔진 제어를 통한 배기가스 저감에 대한 연구

2013년 2월

서울대학교 대학원

기계항공공학부

이 승 현

Study on EGR estimation model by measuring temperatures and reduction of Diesel engine out emission through closed loop control based on the in-cylinder pressure with EGR model

지도교수 민 경 덕

이 논문을 공학석사 학위논문으로 제출함

2013년 2월

서울대학교 대학원

기계항공공학부

이 승 현

이승현의 공학석사 학위논문을 인준함

2013년 1월

위 원 장 김 민 수 (인)

부위원장 민 경 덕 (인)

위 원 송 한 호 (인)

Acknowledgements

First and foremost, I would like to express my respect and gratitude to my advisor, Professor Kyoungdoug Min. During the two years, my knowledge and personality were grown up with his invaluable advices. He gave the inspirations of this study and his guidance and encouragement were the source of power overcoming many difficulties during the project.

I would also like to express my respect and gratitude to Ph.D. Hoimyung Choi from Advanced Institutes of Convergence Technology. I have learned numerous knowledge and know-how about using equipments and engine test through advice of him.

I am very appreciative and very grateful to Seungeun Yu. I could learn about ASCET coding and the Diesel engine combustion control from him. He has always given the valuable ideas and advice.

I would like to special thanks to the project members who offered assistance, valuable discussions and beautiful memories of friendship. Junyong Lee gave many ideas. Seungha Lee, my roommate and colleague, Yoon-woo Lee assisted the engine test. Especially Jeongwoo Lee assisted devotedly without uttering any complaints about heavy workload. Dong-su Kim corrected my awkward English expression. This work would never have been achieved without their efforts and patients.

I would like to present my deepest respect and gratitude to my family. My parents, Jae-kyung Lee and Mun-hee Chae devoted themselves to me with great sacrifice, thoughtful consideration, unimaginable patience, and endless love.

Abstract

Study on EGR estimation model by measuring temperatures and reduction of Diesel engine out emission through closed loop control based on the in-cylinder pressure with EGR model

Seunghyun Lee
School of Mechanical and Aerospace Engineering
The Graduate School
Seoul National University

When Diesel engines operate in the transient state, more emissions are produced than in the steady state. This is due to mismatching between the air-charging system and the fueling system, and the difference in the response time between the intake pressure and the exhaust pressure caused by turbo-lag leads to excess supply of EGR. Since Diesel combustion and its emissions are highly sensitive to the EGR rate, if the precise amount of EGR is known, exhaust gas emissions can be reduced by controlling such parameters as fuel injection timing, injection pressure, etc.

In this study, a model that can predict the EGR rate of the intake gas was developed. In the model, temperatures of the air, the EGR gas and the mixture gas were measured with thermocouples which have a fast response. The EGR rate was calculated through the energy balance equation considering heat transfer.

Moreover, the estimated EGR rate is applied to a closed loop control system which receives feedback from 50% of mass fraction burned (MFB50) for a 2.2 L high speed direct injection (HSDI) Diesel engine. The correction factor of target MFB 50 is affected by the EGR rate. When there is difference between the target EGR and the estimated EGR, the target MFB50 can be retarded or advanced. Cambustion's CLD-500 and DMS 500 were used to measure the NO_x and PM emissions at the transient state. As the air model with the closed loop control is applied to engine control, the emission peak in the transient state was decreased. Especially, the NO_x emission was decreased up to 30 % comparing to that of state without EGR estimation model.

Keywords: Direct injection Diesel engine, Model based control, Closed loop control, Exhaust emission Transient condition

Student Number: 2011-20737

CONTENTS

List of Tables

List of Figures

Acronym

A/F	Air to Fuel ratio
ASCET	Advanced Simulation/Software and Control Engineering Tool
ATDC	After Top Dead Center
BDC	Bottom Dead Center
BMEP	Brake Mean Effective Pressure
BTDC	Before Top Dead Center
CA	Crank Angle
CA50	Crank Angle of 50 % mass fraction fuel burnt
CAI	Controlled Auto Ignition
CAN	Controller Area Network
CI	Compression Ignition
CPS	Crank Position Sensor
DI	Direct Injection
DPF	Diesel Particulate Filter
ECU	Engine Control Unit
EGR	Exhaust Gas Recirculation
EUDC	Extra Urban Driving Cycle
EVC	Exhaust Valve Close
EVO	Exhaust Valve Open
FSN	Filter Smoke Number
HC	HydroCarbon
HRR	Hear Release Rate
HSDI	High Speed Direct Injection
HT	Heat Transfer
IMEP	Indicated Mean Effective Pressure
IQA	Injector Quantity Adjustment

IVC	Intake Valve Close
IVO	Intake Valve Open
LNT	Lean NO_x Trap
LTC	Low Temperature Combustion
MFB50	Mass Fraction Burned 50 %
MIT	Main Injection Timing
MK	Modulated Kinetics
mpg	Miles Per Gallon
NDIR	Non-Dispersive InfraRed Sensor
NEDC	New European Driving Cycle
NO_x	Nitrogen Oxide
NSC	NO_x Storage Catalyst
PID	Proportional, Integral and Derivative
PM	Particulate Matter
RBFN	Radial Basis Function Network
RG	Residual Gas
RGF	Residual Gas Fraction
RPM	Revolution Per Minute
RSM	Response Surface Method
SCR	Selective Catalytic Reduction
SI	Spark Ignition
SoC	Start of Combustion
SoI	Start of Injection
TDC	Top Dead Center
THC	Total Hydrocarbon
TTL	Transistor-Transistor Logic
UEGO	Universal Exhaust Gas Oxygen
VGT	Variable Geometry Turbine

Chapter 1. Introduction

1.1 Research background

1.1.1 Emissions regulations

Diesel engines have been developed constantly. Moreover, the high pressure injection system and air supply system have brought them higher specific power and fuel efficiency. The noise and vibration which are disadvantages of Diesel engines have been decreased. Accordingly, the interest and the market share for them have been increased rapidly for light duty as well as heavy duty. Therefore, the emission regulations of Diesel engines have been strict. These regulations have imposed great pressure on the automotive industries and, hence, much research has focused on means of reducing emissions from vehicles.

However, each country or continent has own standard for the emission of Diesel engines. For example, in Europe, the current emission legislation, Euro 5, restricts the NO_x emission by 0.18 g/km and the soot emission by 0.003 g/km. Furthermore, the number of the PM has been restricted by 6×10^{11} as well as mass since 2011. Euro 6 which will be executed in 2014, restricts the NO_x emission by 0.08 g/km with same level of the PM emission. In the US, Tier2 Bin5 regulation restricts NO_x and

soot emissions by 0.043 g/km and 0.006 g/km, respectively. Due to a characteristic of a Diesel engine, reducing both NO_x and soot emissions requires intensive research since NO_x and soot emissions have trade-off relationship.

1.1.2 Emission characteristics in transient conditions

More emissions are emitted when Diesel engines operate in the transient state than in the steady state. This discrepancy is primarily due to mismatching between the air-charging system and the fueling system and the difference in the response time between the intake pressure and the exhaust pressure caused by turbo-lag. When Diesel engines experience rapid acceleration, the exhaust pressure is immediately increased proportionally to the injected fuel quantity, but the intake pressure is increased relatively slowly because the volume of the intake manifold is larger than the exhaust manifold. This discrepancy leads to a surplus supply of EGR, causing higher PM emissions and fuel consumption due to disrupted combustion in the cylinders. On the contrary, when the engine undergoes a rapid deceleration, the exhaust pressure decreases immediately and the intake pressure slowly follows the target boost pressure. This behavior leads to a shortage of EGR, resulting in higher NO_x emissions. In previous researches, Kang et al. conducted an experiment of

which torque was increased at constant engine speed and engine speed was increased at constant torque. As a result, NO_x emission peak was detected in both cases at low EGR level. Hagena et al. investigated formation of the NO_x emission in transient state, changing the ramp time of load. Increase in the rate of load causes drastically increased NO_x emissions. The sudden change in load produced 1.8 times higher NO_x peak compared to the load change in 5 seconds.[1-7]

1.1.3 Application of combustion control

Control of modern Diesel engines involves a large number of parameters, such as the start of injection, the EGR rate, the injection pressure, the fuel quantity, etc. These parameters must be controlled for the engine to be operated in an optimal state. Some of these parameters are controlled in open-loop control and others are controlled in closed-loop control mode.[8] Open-loop control provides fast response and relatively easy control. However, it cannot handle changes in the state caused by variation in conditions such as aging of the injectors and fuel quality. On the other hand, closed-loop control monitors the present state so that any changes in conditions can be considered in the control mechanism. For Diesel engines, many studies have utilized closed-loop control with the closed loop collecting combustion state information as feedback. Combustion state information can be obtained directly from the in-cylinder pressure or indirectly from the combustion noise and

vibration. For an indirect method, an accelerometer is used to measure vibration from the engine head or the surface of blocks and information can be obtained from these signals. This method is economically affordable due to the fact that combustion information of multi cylinders can be extracted by one accelerometer but obtainable information is limited and signals can be distorted by any noise source [9-13]. Using the in-cylinder pressure is the most reliable method as well as a direct method. The rate of heat release (RoHR) can be calculated from the pressure data, and then a combustion parameter of interest, such as the 50 % mass fraction burned (MFB50), start of combustion (SOC) or the location of peak pressure (LPP), can be calculated from the RoHR. The control parameters are adjusted to set a target value for the combustion parameters.[14,15,16]

1.1.4 Real-time EGR estimation

As mentioned above, in the transient state, unexpected changes in the EGR rate due to fluctuation of pressure difference between intake and exhaust ports lead to higher emissions than in the steady state. If the accurate EGR rate can be estimated and be accounted for in engine control, then emissions can be reduced. Many studies have suggested a mean value model to estimate the exact EGR rate. In previous research, Park et al. developed the cylinder air charge model based on the volumetric efficiency and the measured pressure of the intake manifold. In this method, the

model for the turbocharger and volumetric efficiency for the intake manifold geometries has to be made. In addition, the model for the EGR valve, the swirl valve and the throttle are need as well. This method attains good accuracy but the calculation is complicated and the model has to be modified according to engines. [17] Desantes et al. and Mladek et al. developed models using the in-cylinder pressure. After intake valve close (IVC), the gas is under adiabatic compression. If the difference in the pressure at two moments during the compression process and the in-cylinder temperature at one moment are known, then the mass of the gas can be calculated. This method has an advantage of simple calculation. However, measuring the pressure difference accurately is very hard due to bias errors in the signal. Moreover, to estimate the temperature is inaccurate due to many assumptions. The temperature strongly depends on atmospheric temperature, boost pressure, compressor efficiency, intercooler efficiency, exhaust manifold temperature, EGR cooler efficiency and EGR rate. On the other hand, the residual gas fraction and heat transfer from the block which are also the important factors depend on the operating conditions. [18,19] Yu et al. measured in-cylinder pressure at IVC and estimated T_{IVC} from the T_{EGR}, T_{air} and heat transfer correction factor to predict EGR rate. This method also has similar weakness because the pressure data and assumptions are needed as well. Furthermore, the used conventional commercial air flow meters which are installed in the intake air duct are inaccurate. The error affects the

estimation directly.

1.2 **Objective and expected benefits**

The objective of this study is to develop an EGR prediction model using fast response temperature measurements at the intake manifolds. The heat transfer at the intake port is considered to improve the accuracy of the model. Moreover, the EGR prediction model is applied to MFB 50 control logic for reducing NO_x peak caused by lack of EGR when engine speed and load are decreased sharply.

In this paper, a Diesel engine was controlled with a closed-loop control system adapted to MFB50 feedback. When the difference between the target EGR rate, which was set in the steady state, and the estimated EGR rate is above a certain threshold, a correction factor is added to the target MFB50. The corrected MFB50 is varied within a range where IMEP loss can be minimized and this could change SOI, resulting in reduction in NO_x emissions when engine speed and load are decreased rapidly.

Chapter 2. Experimental Apparatus

2.1 **Overall configuration**

Figure 2.1 shows the schematic diagram of the experimental apparatus for this research. The experimental apparatus consists of the engine, exhaust gas analyzers, combustion control system and temperature measuring system for EGR rate estimation.

2.2 **Multi-cylinder Diesel engine**

A 2.2 L 4-cylinder turbocharged Diesel engine shown in Figure 2.2 which was developed by HMC was used in this research. The piezoelectric type injectors and high pressure fuel injection system of Bosch which enable injection pressure up to 1600 bar were equipped. The engine was controlled by ECU of Bosch, which can communicate by ETK protocol and their variable was able to be monitored and bypassed. Detailed specifications of the engine are shown in Table 2.1.

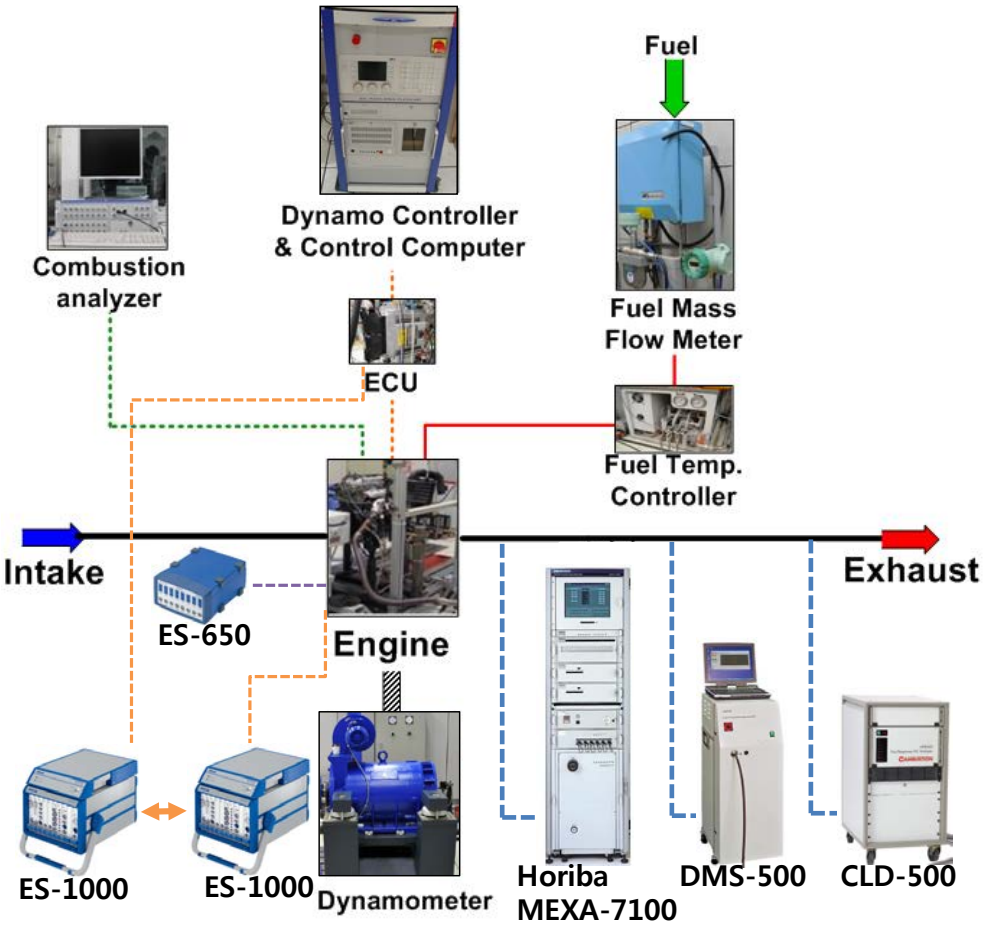

Figure 2.1 Schematic Diagram of Experimental Equipment

Figure 2.2 4 cylinder 2.2 L Diesel engine

Table 2.1 Specifications of engine

Criteria	Specification
Layout	In-line 4 cylinder 2.2 L
Max power	200 hp / 3800 RPM
Max torque	44.5 kgm / 1800 RPM~2500 RPM
Bore	85.4 mm
Stroke	96 mm
Displacement volume	550 cc
Connecting rod	145 mm
Compression ratio	16
Valve timing	IVO : 10° BTDC
	IVC : 28° ABDC
	EVO : 54° BBDC
	EVC : 4° ATDC
Fuel injector type	Piezoelectric type
ECU version	EDC 17C

2.3 **Engine test equipment**

The engine was connected to a 340kW AC transient dynamometer (AVL, PUMA). The transient dynamometer can control engine speed and torque in real-time by measuring the engine speed and torque so that the engine can be tested in dynamic driving test mode e.g. NEDC and FTP-75. Detailed specifications of the dynamometer are shown in Table 2.2.

The coolant temperature was controlled to maintain 85°C during the engine test using the water-cooled coolant temperature controller (SAMBU, SWC-1200). To maintain uniform quality of the fuel during the experiment, the fuel was supplied from the 4000 liter tank and the temperature of the fuel was controlled to keep 40°C by using the fuel temperature controller (SAMBU, SFTC-1400). The cetane number of the fuel was 53. The engine test cell temperature was controlled to 25 ℃ by an air-conditioning system and the temperature of the fresh air which was supplied to engine was maintained at 25 ℃.

2.4 **Exhaust gas analyzer**

2.4.1 Exhaust gas analysis in steady state

In the steady state, the concentrations of the CO2, CO, O2, NO_x and THC of the engine out exhaust gas were measured by a Horiba MEXA 7100 DEGR. The concentrations of the CO and CO2 can be measured by NDIR method and the concentrations of NO and NO_x were measured by CLD method. Other specific information is in the Table 2.4. The analyzer can measure CO2 concentration at two points. The EGR rate can be calculated by measuring CO2 concentration in exhaust manifold and intake manifold simultaneously. The AF ratio can be calculated by using other gases concentration.

The PM was measured by an AVL Smokemeter 415S. It operates by drawing a known and variable volume of exhaust gas through a paper filter. The reflectance of the paper is measured to determine the paper blacking and calculation of the smoke level in Filter Smoke Number (FSN). It has good correlation with mg/m^3 but the time resolution is approximately 1 min. The other specific information is shown in Table 2.3.

2.4.2 Exhaust gas analysis in transient state

The objective of this research is estimating the EGR rate in real-time and applying the EGR model to engine combustion control to reduce the engine out emissions. To verify the effects of the control, the NO_x emission was measured by CLD-500 and the PM emission was measured by DMS-500 in real time.

2.4.2.1 CLD-500

As the response time of conventional CLD devices is about several seconds, it is not suitable to measure the NO_x during transient states. During response time of a conventional CLD, an engine will undergo many firing cycles. Accurate temporal measurement of NO_x is provided by a CLD 500 Fast NO_x analyzer. It is a chemiluminescent detector that is used for measuring NO and NO_x concentration in a sample gas and has a 90%-10% response time of less than 3 ms for NO [10] and less than 10 ms for NO_x [11]. This is achieved by locating the detectors in remote sample heads that are positioned very close to the sample point in the engine and conveying the sample gas to the detectors under the influence of a vacuum through narrow heated capillaries. This allows the CLD500 to distinguish between two adjacent firing cycles, and even offer information about the variation in NO concentration during a single exhaust stroke. Other specifications are in Table 2.5.

2.4.2.2 DMS-500

Temporally resolved particulate concentrations are provided by a differential mobility spectrometer DMS-500 manufactured by Cambustion. This instrument measures the number of particles and their spectral weight in the size range of 5 nm to 1000 nm with a time response of 200 ms. The instrument provides aerosol size spectral data by using a corona discharge to place a prescribed charge on each particle. The charged particles are then introduced into a strong electrical field inside a classifier column as shown in Figure 2.3. This field deflects the particles away from the electrode through a sheath flow toward the electrometer detectors. Particles with lower aerodynamic drag-to-charge ratio will deflect more quickly and are attracted towards electrode rings closer to the beginning of the classifier column, and vice versa. Classification of small particles in this manner is very effective because the electrostatic force is very high relative to any others. As the particles land on the grounded rings, they release their charge and these outputs from the electrometers are processed in real time to provide spectral data and other desired parameters. Other specifications are in Table 2.6.

Table 2.2 Specifications of dynamometer

Item	Specfication
Manufacturer	AVL ELIN
Model	MCA-231
Capacity	190 kW
Type	AC
Maximum rpm	6980 rpm
Cooling	Air cooling

Table 2.3 Specifications of smoke meter

Item	Specification
Manufacturer	AVL
Model	AVL 415S
Measurement range	0 ~ 10 FSN / 0 ~ 32,000 mg/m³
Resolution	0.001 FSN / 0.01 mg/m³
Repeatability (as standard deviation)	$\sigma \leq \pm$(0.005 FSN + 3 % of measured value)
Reproducibility (as standard deviation)	$\sigma \leq \pm$(0.005 FSN + 6 % of measured value)

Table 2.4 Measurement principle of emission analyzer (MEXA-7100DEGR)

Emissions	Measurement principle
NO_x	Chemiluminecent Detector
THC	Flame Ionization Detector
O_2, CO_2, CO	Non Dispersive Infrared Rays

Table 2.5 Specifications of fast response NO_x analyzer

Item	Specification
Manufacturer	Cambustion
Model	CLD-500
Measurement range	0 ~ 100 ppm to 0 ~ 20,000 ppm
Linearity	±1 % FS to 5,000 ppm ±2 % FS to 10,000 ppm
Response time	2 ms (10 ms with NO_2measurement)
Zero stability	5 ppm for 1 hour

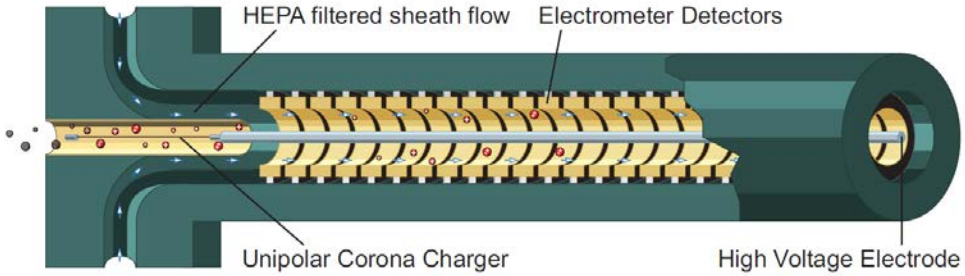

Figure 2.3 Operating principle of DMS-500

Table 2.6 Specifications of DMS-500

Criteria	Specification
Particle Size Range	5 nm – 1 µm (5 nm – 2.5 µm option)
Number of Electrometers	22
Size Classification	Electrical Mobility
Dilution Factor Range	÷ 1 – 3000
Maximum Primary Dilution Temperature	150 °C
Sample Flow rate	8 slpm (1 µm range) at 0 °C + 100 kPa
Instrument Zeroing	Automatic; internal HEPA filter
Spectral Elements	16 or 32/decade
Output Data Rate	10/sec – 1/min
Time Response	$T_{10-90\%}$ 200 ms $T_{10-90\%}$ 300 ms with 5m heated line
Calibrations: Non-agglomerate: Agglomerate (Diesel):	By NIST traceable PSL spheres & DMA size selected NaCl/H SO , comparison with standard electrometer DMA size selected soot, comparison with standard electrometer
Calibration Interval	12 months
Max Concentration	≈10_{11} dN/dlogD /cc (diluter on)

2.5 **Combustion control system**

In this research, the developed EGR estimation model was applied to closed loop engine combustion control to reduce NO_x in transient. The closed loop engine combustion control system adjusted the SoI receiving the feedback from MFB50. This control system consists of combustion analyzer and combustion controller. The MFB50 was calculated form RoHR which was calculated in combustion analyzer from receiving the in-cylinder pressure and crank angle data. The calculated value can be sent to combustion controller by CAN IO, so the controller set the proper SoI. The combustion controller and combustion analyzer were programed in each ES1000, rapid control prototype. Figure 2.6 shows the schematic diagram of the closed loop control system.

2.5.1 ES1000

Each ES1000 consists of some modules. Both have the ES1231.1 which is the rapid control prototype module. The module has the single core processor and ASCET code is used. Moreover, both have CAN IO module in order to communicate each other. The ES1000 for combustion analyzer has AD module to receive the signal of in-cylinder pressure and crank angle. The ES1000 for the combustion controller has the ETK communication module to communicate with

ECU. The variables of the ECU can be monitored and bypassed via ETK communication. The specific information was listed in Tables 2.7 and 2.8.

2.5.2 Combustion pressure measurement

The in-cylinder pressure was measured by a piezoelectric type pressure sensor manufactured by Kistler. The sensor can measure pressure up to 250 bar. Other specifications can be found in the Table 2.9.

Using the glow plug type adaptor, the pressure sensor can be installed in-cylinder without modifying the head or block of the engine. The adaptors have different shape according to Engine. The Figures 2.4 and 2.5 show the adaptor and pressure sensor.

The fine charge from the pressure sensor was amplified and converted to voltage by charge amp. The used amp was type 5063A module of SCP type 2853A. Other specifications are on Table 2.10.

Table 2.7 Specifications of combustion analyzer

Criteria		Specification
Simulation Board	CPU	1 GHz
	RAM	256 MB SDRAM
A/D board		16 CH, 100 kHz/CH
D/A board		8 CH
Digital and PWM I/O board	Channel	16 CH input, 16 CH output 2 external trigger
	Frequency	1 Hz to 60 kHz
CAN Communication		4 CAN signal

Table 2.8 Specifications of combustion control logic

Criteria		Specification
Simulation Board	CPU	1 GHz
	RAM	256 MB SDRAM
CAN Communication		4 CAN signal
ETK Communication		1 CH, 100 MBit/s

Table 2.9 Specifications of the pressure sensor

Criteria	Specification
Measuring range	0 ... 250 bar
Sensitivity	≈−20 pC/bar
Natural frequency, nominal	≈160 kHz
Linearity in all ranges (at 23 ° C)	≤ ±0,3 %/FSO
Acceleration sensitivity	<0,0005 bar/g
Operating temperature range temperature min./max.	−20 ... 350 −50 ... 400 ° C
Sensitivity shift 200 ± 50 ° C 23 ... 350 ° C	≤ ±0,5 % ≤ ±2 %
Insulation resistance at 23 ° C	≥1013 Ω
Shock resistance	2 000 g
Capacitance, without cable	5 pF

Table 2.10 Specifications of the charge amp

Criteria	Specification
Measuring range I	±5,000 ...±50,000 pC
Measuring range I on delivery	±20,000 pC
Error	<±1 %
Drift (0 ... 50 ° C)	<±0,2 pC/s
(25 ° C) Frequency range (20 Vpp) Reset/Operate transition	<±0,05 0 ... >25 <±2 pC/s kHz pC
Max. voltage between sensor GND and output/ supply voltage	<±50 V
Suppression of the interference	>70 dB
Output voltage	0 ... ±10 V
Output current	0 ... ±2 mA
Output resistance	10 Ω
Output interference signal (0,1 Hz ... 10 MHz)	<10 mVpp

Figure 2.4 Pressure sensor

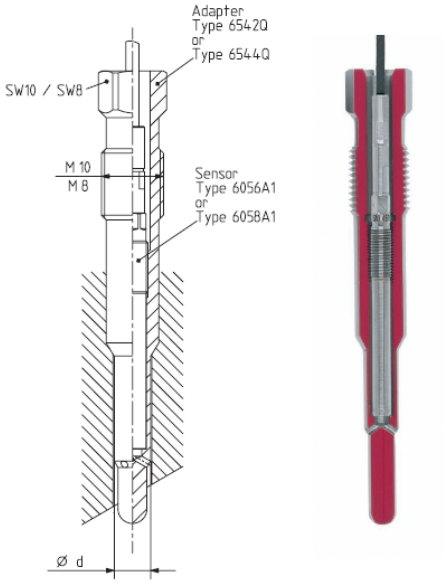

Figure 2.5 Glow plug type adaptor

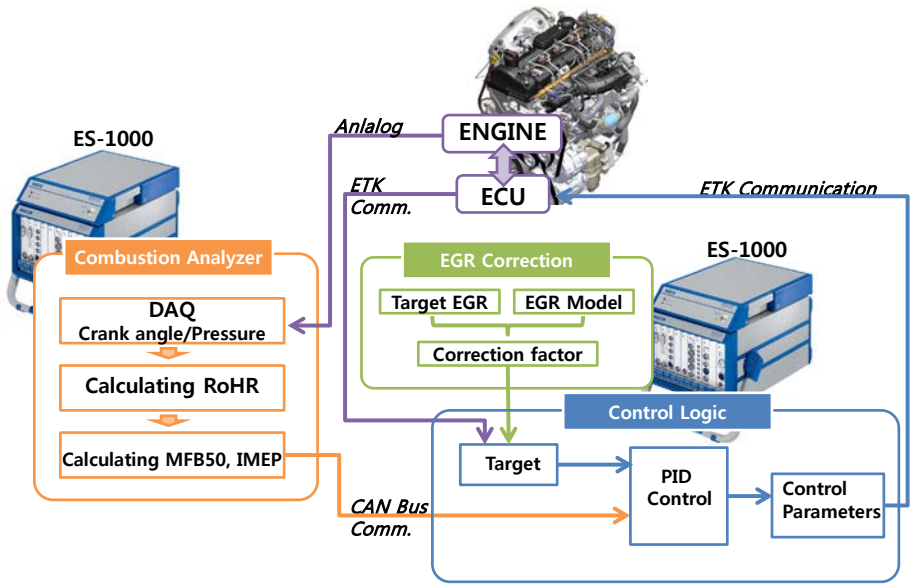

Figure 2.6 Schematic diagram of the closed loop control system

2.6 **Temperature measuring system**

In this research, model of EGR rate estimation was developed using temperature measurement. The temperature was measured by R-type thermocouples. These thermocouples are exposed type with 50 μm diameter, so they have fast enough response times, less than 100ms, to measure temperature variation during the transient state. The thermocouples are connected to ES650, which has thermocouple amplifiers and AD converters. The signals from the ES650 can be monitored and logged using the software package INCA and the sample rate is 10 Hz. Table 2.11 shows specifications of the ES650.

Table 2.11 Specifications of ES650

Criteria	Specification
Resolution	21 bits; corresponding to 0.01 K for J-, K and N-type thermocouples
Sampling rate	0.1 to 10 samples/sec, configurable for each channel
Measuring range	-50 to +1768 ° C (type R)
Cutoff frequency	10 Hz
Input impedance	> 10 MΩ ‖ 10 nF
Maximum inaccuracy	0.050 % + 2.0 K for type R
Maximum temperature drift	±0.0400 K/K for type R
Maximum inaccuracy ΔTi depending on the internal resistance of the thermocouple at internal resistances > 50 Ω	±0.0300 K/Ω for type R
Maximum inaccuracy of cold junction	±1 K
compensation ⊿Tcjc	

Chapter 3. Real-time estimation algorithm of engine operating conditions based on in-cylinder pressure

3.1 Overall logic description

The engine was controlled in the closed loop control that has MFB50 and IMEP feedback. For the system, two of rapid control prototypes (RCP) were used. The schematic diagram of the control logic is shown in Figure 2.6. One of them provided combustion information calculating the RoHR and the other controlled the engine. They communicated by CAN Bus. The RCP controlling engine had engine control logic and communicated with the ECU by ETK. It collected the information of ECU, such as SOI and intake pressure and controlled engine by overwriting the information on ECU such as SOI and fuel quantity. The other RCP which had combustion analyzer logic received data of the a crank position sensor and in-cylinder pressures sensors to calculate MFB50 in real-time.

3.2 Combustion analyzer

In order to analyze the combustion in the cylinders, information of the crank angle was acquired from the crank angle position sensor that was installed in the engine

and the pressure data was acquired from the DAQ board included in RCP. The CPS was 60-2 type and one tooth of them was 6 degrees. To improve the resolution, the imaginary signal was produced from the CPS data by 1 degree. The in-cylinder pressure was acquired by 20 kHz and was interpolated by 1 degree at every crank angle. The RoHR was calculated from the data. The window for the calculation of RoHR was between 40º BTDC and 90º ATDC. The MFB50 was obtained by accumulating the RoHR. For real-time application, the calculation has to be completed before the next cycle starts to utilize the MFB50 and IMEP feedback data at each cycle. Moreover, the time to calculate the control input from the feedback and the time to overwrite the ECU data with values must be sufficiently low. For the control logic to be punctual, time scheduling is absolutely crucial. Figure 3.1 shows the time scheduling of the logics. The calculation of the RoHR starts at 90º ATDC and is scheduled to finish before 270º ATDC. The calculation of the MFB50 follows in the next 90 CA. The input values of the control parameter, such as the SOI, are calculated between 270º BTDC and 180º BTDC, and the values are saved in ECU data until 90º BTDC. Time scheduling is based on crank angles because the required time differs as the rpm changes. This combustion analyzer logic is feasible up to 3800 rpm.

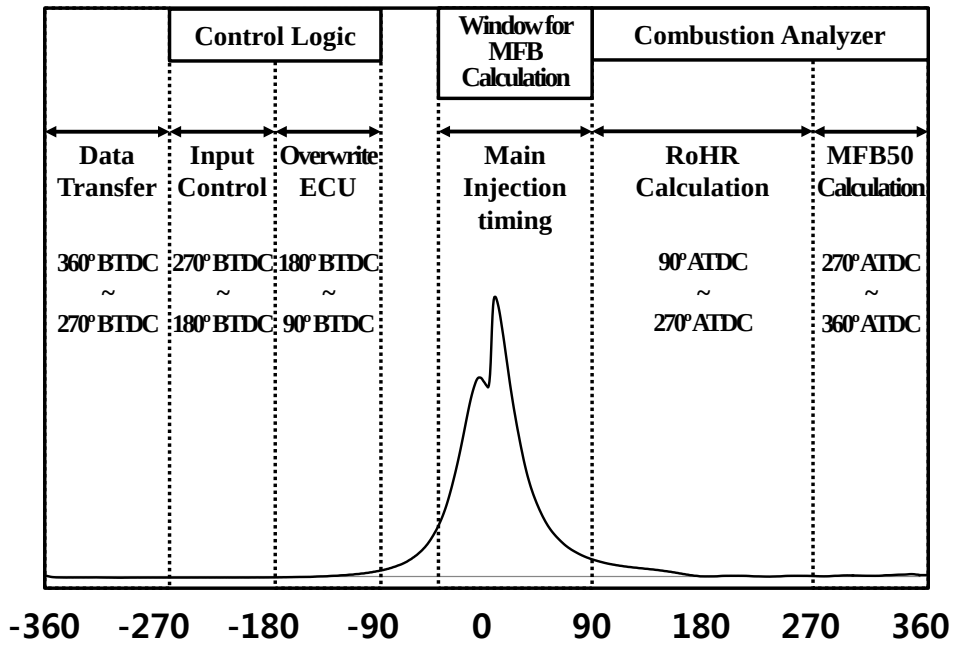

Figure 3.1 Time scheduling of the control logics

3.3 **Combustion control logic**

In this work, the combustion control logic is operated in closed loop. The MFB50 is monitored and the control inputs are controlled to force the MFB50 to follow the target value. The MFB50 is affected by the EGR rate, the pilot injection timing, the main injection timing, the rail pressure, etc. However, in this study, the main injection timing is adjusted to control the MFB50 because the main injection timing is nearly linearly proportional to the MFB50.[16] The PID controller is designed to cause the present MFB50 to approach the target value. The PID gain is determined according to the rpm and the injected fuel quantity. The change in the main injection timing is limited to ensure the system's stability. The target MFB50 is a 2-dimensional map that varies according to rpm and fuel quantity. The map's values are determined from steady-state experiments. In addition, a correction factor for the coolant temperature is added to the target value because the coolant temperature significantly affects in-cylinder combustion. IMEP was controlled similar to the MFB50 control. The target values were determined from the steady-state experiments and the values were composed of 2-dimensional map by engine speed and fuel quantity. The PID controller was designed for adjusting the fuel energizing time to make the present IMEP follow the target value. The correction factor for the coolant temperature was included because the target values have to be modified in

cold start state

3.4 **EGR correction factor for closed loop control**

In the transient state, the unexpected change in the EGR rate leads to higher emission levels. In detail, when the engine undergoes rapid deceleration, a shortage of the EGR occurs due to the slow response of the air-charging system, and hence more NO_x is emitted. To reduce NO_x emission, a correction factor for EGR should be included in MFB50 control. The correction factor is determined by the difference between the target EGR rate and the current EGR rate values. The current EGR rate was estimated by the model which was developed and using the measured temperatures with considering the heat transfer. The target EGR value was pre-determined by the experimental results at the steady state. These values were formed into 2D map in accordance with rpm and BMEP. When there is a little difference in EGR rate, if the correction factor is applied, it would be effective in NO_x reduction but there can be a loss in IMEP. Therefore, the correction factor is only applied when the difference in EGR is over the threshold value where a large NO_x peak is expected. Furthermore, limit was set for the correction factor to prevent a great deal of loss in IMEP caused by largely retarded target MFB50 due to sudden and big difference in EGR.

Chapter 4. EGR RATE ESTIMATION USING TEMPERATURE MEASUREMENT

4.1 EGR rate estimation using the energy balance equation

The EGR rate of Diesel engines can usually be determined by measuring the concentrations of CO2 in the intake manifold, the exhaust manifold and the air. The industrial standard method for measuring CO2 is NDIR (Non-Dispersive Infra-Red). The response time of conventional analyzers is approximately 3~5 seconds, which is too slow to measure the change of the EGR rate during the transient state at the intake manifold. [20]

Han et al. measured the EGR rate by measuring the temperatures of the air, the EGR gas and the gas in the intake manifold using a fast response hot wire. The response time was fast enough to measure the EGR rate during the transient state. The EGR rate was calculated using equation (1). The specific heat capacity of the air and the EGR were assumed to be the same and heat transfer was neglected. [21]

$$\mathrm{EGR} = \frac{m_{EGR}}{m_{EGR}+m_{air}} = \frac{T_{mix}-T_{air}}{T_{EGR}-T_{air}} \quad (3\text{-}1)$$

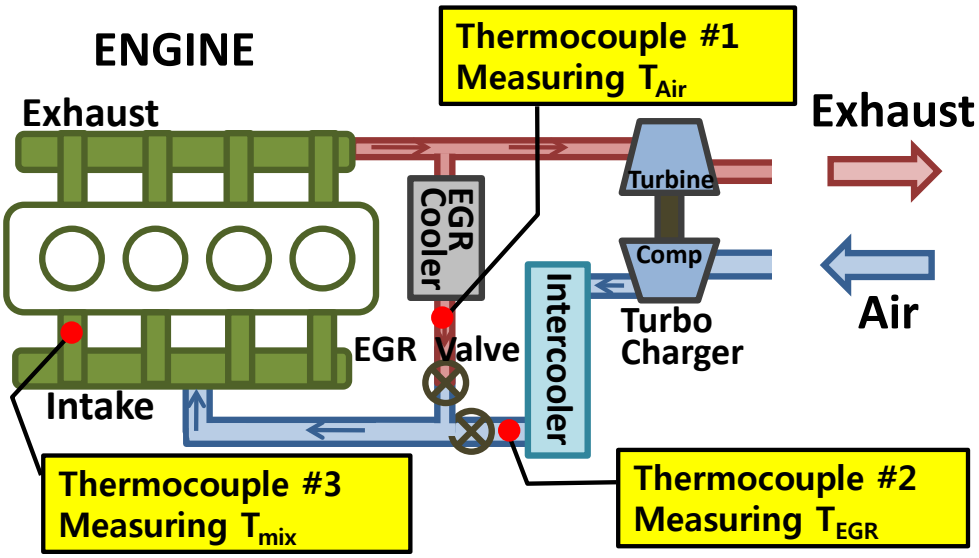

Figure 4.1 Schematic diagram of temperature measuring spots

4.2 **Validation the EGR model**

The experiment was executed from 1000 rpm and 2 bar to 2000 rpm and 6 bar by changing the EGR rate at each rpm and load. The experimental cases are shown in Table 4.1. The temperature of the air was measured at downstream of the intercooler. The temperature of the EGR gas was measured at downstream of the EGR cooler. The temperature of the mixture was measured at close to the 1st cylinder as shown in Figure 4.1 to estimate the EGR rate of the 1st cylinder.

Figure 4.2 shows the verification results of the EGR estimation without considering heat transfer from the intake manifold wall. The X axis is the EGR rate measured using the NDIR method by the Horiba MEXA-7100 and the Y axis is the EGR rate calculated by the model using the temperatures. When the heat transfer was not considered, and the less EGR gas was entered into the cylinders, the larger errors occurred. While the EGR rate measured by exhaust gas analyzer was 0 %, the EGR rate estimated was about 8 %. It is because $T_{mix}$was not the same as T_{air} but it was 2 ~ 3 ℃ higher, due to heat transfer from the intake manifold. The intake manifold is colder than the EGR gas and hotter than the intake air, which is cooled in the intercooler, the EGR gas will lose heat to the intake manifold and the air will gain heat from the intake manifold.

Table 4.1 The experimental cases for verification of EGR model using the temperatures

speed [rpm]	load BMEP [bar]	Target EGR %
1000	2	37, 25, 20,10,0
1250	2	36, 25, 20, 10,0
1500	4	29, 20, 10,0
1750	6	20,10,0
2000	6	20,10,0

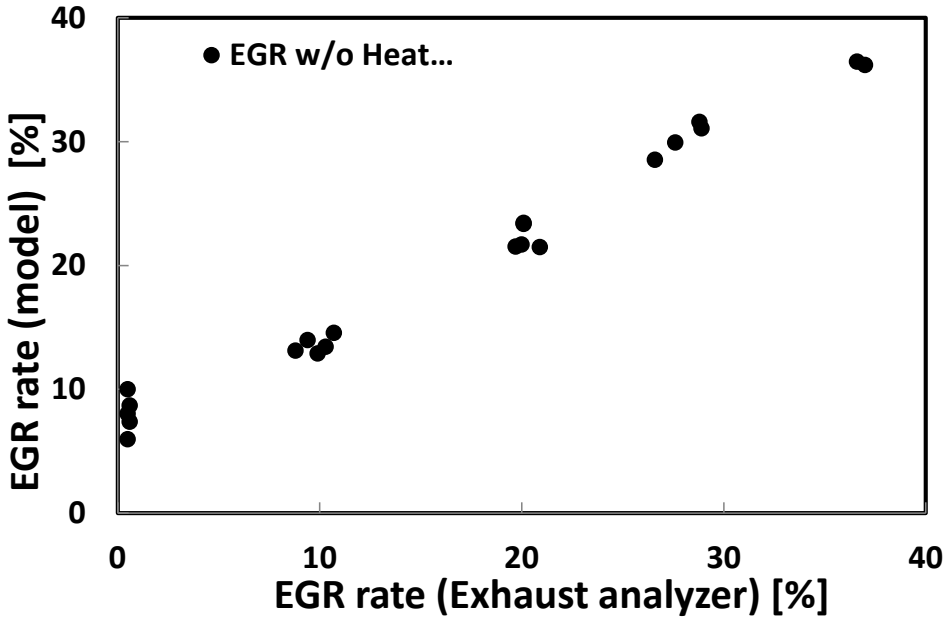

Figure 4.2 The verification of EGR estimation model without heat transfer

4.3 **EGR model considering the heat transfer**

If T_{mix} is changed up by 3 ℃ due to heat transfer, the error is up to 5 % of EGR rate. That is why the heat transfer has to be considered. Thus, we developed the EGR model using the temperature of air, EGR gas and the mixture, which includes heat transfer model in the intake manifold. The heat transfer is treated as follows. Assuming there is no heat transfer,

$$\dot{H}_{mix} = \dot{H}_{air} + \dot{H}_{EGR} \tag{4.1}$$

$$c_p \dot{m}_{mix}(T_{mix,noHT} - T_0) = c_p \dot{m}_{air}(T_{air} - T_0) + c_p \dot{m}_{EGR}(T_{EGR} - T_0) \tag{4.2}$$

$$T_{mix,noHT} = T_{air} - EGR \times T_{air} + EGR \times T_{EGR} \tag{4.3}$$

If the effect of heat transfer is taken into account,

$$\dot{H}_{mix} = \dot{H}_{mix} + \dot{Q}_{in} + \dot{H}_{EGR} + \dot{Q}_{out} \tag{4.4}$$

$$\begin{aligned} c_p \dot{m}_{mix}(T_{mix,HT} - T_0) &= c_p \dot{m}_{air}(T_{air} - T_0) + c_p \dot{m}_{EGR}(T_{EGR} - T_0) \\ &+ hA_{air}(T_{wall} - T_{air}) - hA_{EGR}(T_{EGR} - T_{wall}) \end{aligned} \tag{4.5}$$

$$T_{mix,HT} = T_{air} - EGR \times T_{air} + EGR \times T_{EGR} + h[A_{air}(T_{wall} - T_{air}) - A_{EGR}(T_{EGR} - T_{wall})] \tag{4.6}$$

$$T_{mix,HT} = T_{mix,noHT} + \Delta T \tag{4.7}$$

$$\Delta T = h \frac{h}{c_p \dot{m}_{mix}} [A_{air}(T_{wall} - T_{air}) - A_{EGR}(T_{EGR} - T_{wall})] \tag{4.9}$$

$$\mathrm{Re} = \frac{\rho v D}{\mu} \tag{4.10}$$

Where H_{air}, H_{EGR}, H_{mix} are the enthalpies of the air, the EGR gas and the mixed gas, respectively. $c_{p,air}$, $c_{p,egr}$, and $c_{p,mixed}$ are the specific heat capacity at constant pressure of the air, the EGR gas and the mixed gas, respectively. Q_{in} is the heat that the air gains and Q_{out} is the heat lost by the EGR gas. T_{air}, T_{EGR} and T_{mix} are measured values. Equation (4.2) represents the mixture temperature without considering the heat transfer and equation (4.5) represents the mixture temperature with the heat transfer. Increase in the temperature by the heat transfer which is represented in equation (4.8) can be obtained by subtracting equation (4.2) from equation (4.5).Heat transfer coefficient of h can be obtained from Nu and the intake manifold was assumed to be a pipe. Nu is obtained from Re which is a function of pressure, rpm and geometry of the intake manifold. Also, it is assumed that the heat transfer from the wall can only affect ΔT. The heat transfer by radiation was ignored due to surrounding temperature. [22]

Thus, the EGR rate can be calculated from equation (3.1) by T_{air}, T_{egr} and $T_{mix,heat}$ are measured by thermocouples. The used thermocouple whose diameter was 100 μm is an exposed type and the response time was 0.05 s. [23] Temperature data was acquired by ES650 and the sampling rate was measured to be 10 Hz.

The calculated EGR rates by the model including the heat transfer were shown in Figure 4.2. When heat transfer was considered, the estimated EGR rate was in good agreement with the EGR rate measured using the NDIR method. The coefficient of determination was 0.996

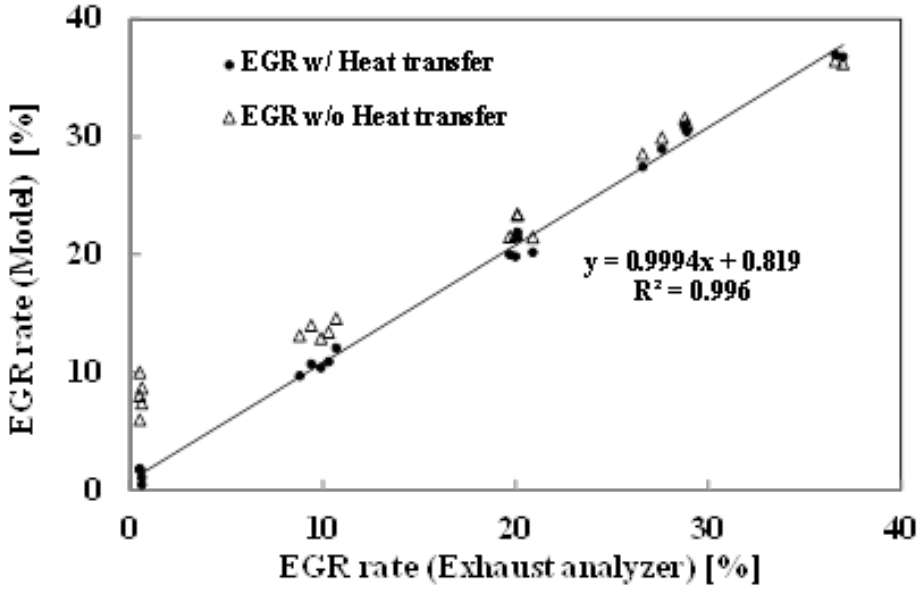

Figure 4.3 The verification of EGR estimation model with heat transfer

4.4 Analysis EGR model in ECU

For Diesel engines, relatively large amount of EGR is supplied via external loop to reduce NO_x emissions. It is important to control the amount of EGR rate since it affects NO_x and PM emissions, and fuel consumption. Therefore, a model which estimates the EGR rate is included in ECU for conventional Diesel engines. The model is a filling emptying type model which is related with volumetric efficiency and openness of the EGR valve. Well-tuned EGR model can achieve good results at the steady state but, for the transient state, it is not quite so.

Figures 4.4~4.6 represent the EGR rate estimated by ECU model and developed model in the transient state. The engine was decelerated from 1750 rpm 8 bar to 1250 rpm 2 bar in 3 seconds as shown in Figure 4.4. At that time, the EGR rate from the ECU and EGR rate from developed model using temperatures are shown in Figure 4.5. EGR valve openness and air flow rate from the ECU are displayed in Figure 4.6. At 2 seconds, deceleration starts and, at this time, EGR valve openness is increased to compensate temporal lack of EGR. However, EGR rate from the ECU decreases and approaches to 0 %. At that time, EGR rate from the model using temperature measurement shows the same decreasing tendency but the minimum value is maintained as 5 %.

This error is due to the inaccuracy of the air flow rate. Figure 4.6 represents

sudden increase in the air flow rate from the ECU. At this state, the total amount of in-cylinder air calculated by ECU is larger than the amount of in-cylinder air measured by the flow meter, so the EGR rate value becomes negative. Nevertheless, it is not physically possible that EGR rate is lower than 0 % and, hence, it is represented as 0 %. Fluctuation in the flow meter is very large as it can be shown in Figure 4.6. For many researches for EGR estimation models, improving accuracy of the model is difficult due to inherent inaccuracy of air flow estimation on engines.

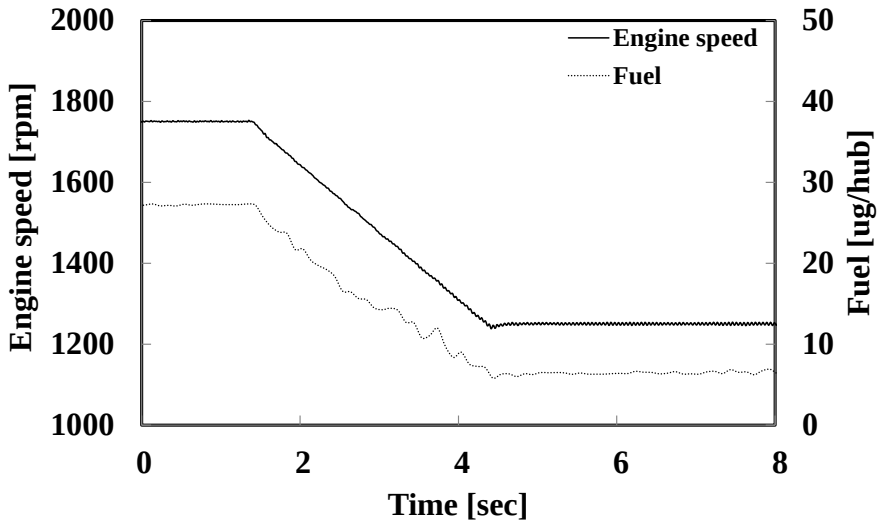

Figure 4.4 Engine speed and injected fuel quantity / EGR model in ECU of conventional Diesel engines in transient state

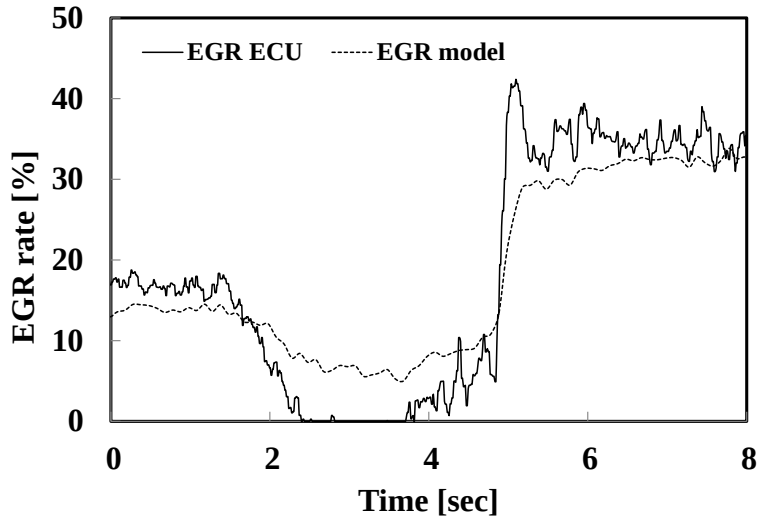

Figure 4.5 EGR rate from ECU and from model / EGR model in ECU of conventional Diesel engines in transient state

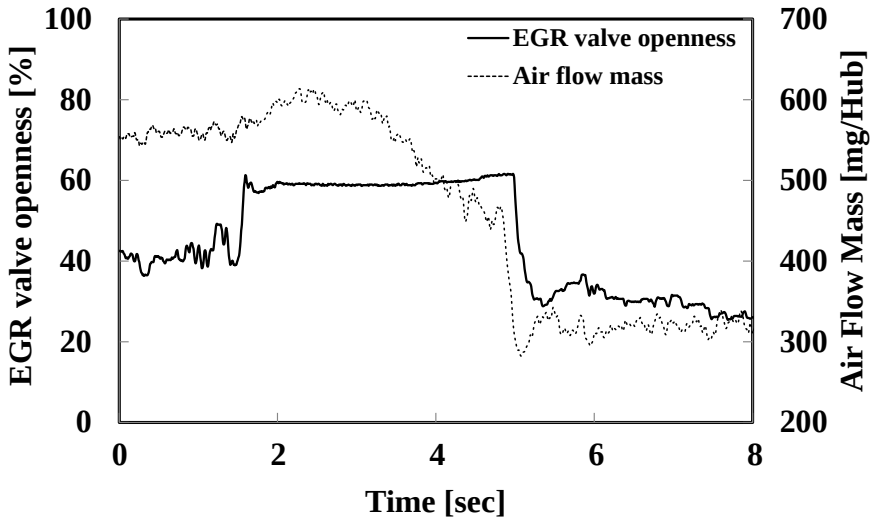

Figure 4.6 EGR valve openness and air flow mass / EGR model in ECU of conventional Diesel engines in transient state

Chapter 5. Result and Discussion

The EGR rate and NO emissions were examined in the rapid deceleration state. The engine speed was varied from 1750 rpm to 1250 rpm and the load was varied from BMEP 8 bar to BMEP 2bar over 3 seconds as shown in. Figure 5.1. Figure 5.2 displays the target value and measured value of intake pressure. The target value and the present EGR rate estimated by the model are represented in Figure 5.3. When the speed and load decrease, the target EGR rate increases. However, the present EGR rate instantaneously decreases. As shown in Figures 5.1 and 5.2, the intake pressure was higher than target value. It is because the response of the intake pressure is slower than the response of the exhaust pressure due to the difference of the volume between intake manifold and exhaust manifold. Thus, more air flows into the cylinder, the EGR will be starved and the NO_x emission will increase beyond the steady-state value. Figure 5.4 shows the NO and PM emissions measured using the CLD500 and the DMS500, respectively. The NO peaked up to 320 ppm when the EGR rate dropped below the target EGR rate during the decrease in the engine speed and load, despite the NO emission level was changed from 200 ppm to 80 ppm in the steady state. 160 % more NO emission was emitted during the transient, thought PM emissions slightly decreased than the steady state, because more air was trapped in the cylinder.

In the rapid deceleration state, NO emissions will decrease if the SOI timing is retarded. This study employs a closed-loop control scheme in which the SOI timing is adjusted to reduce the difference between the target MFB50 and the present MFB50. Moreover, the logic includes the EGR correction factor, which retards the target MFB50 timing when the difference between the target EGR rate and the EGR rate estimated using the EGR model exceeds a threshold.

As shown in Figure 5.5, after 4 seconds at which the engine started deceleration, the gap between target EGR and present EGR is increasing. When the difference is over the threshold, the correction factor added to target MFB50. As the target MFB50 delayed, the SOI was retarded as shown in Figure 5.6. If the difference is larger than the limit, the limit logic will work, and the correction factor will be fixed to a constant value to improve the stability of the system. As the result of employing the EGR correction logic to MFB50 control logic, the NO peak disappeared and the level was similar to level in the steady state as shown in Figure 5.7. The slight decrease in PM emission level was also similar to level in the steady state.

When the target MFB50 is retarded, the IMEP and BSFC could become worse. However, we just focus the rapidly decelerate state in which the load of engine is not needed.

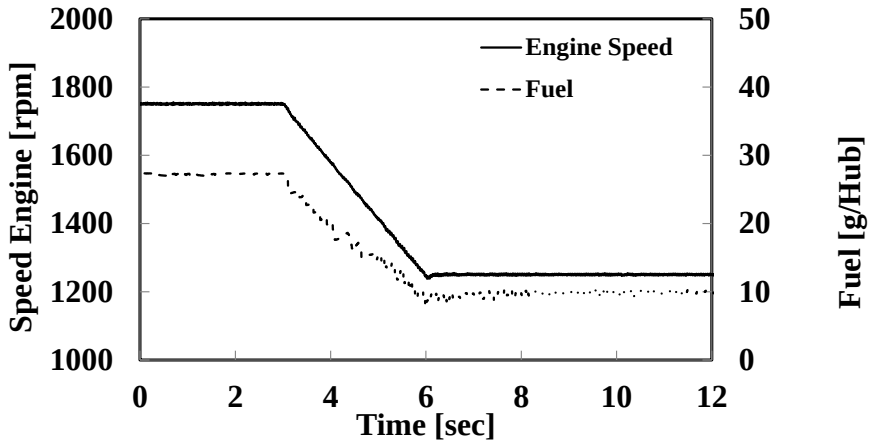

Figure 5.1 Engine speed and injected fuel quantity in transient state without EGR correction logic

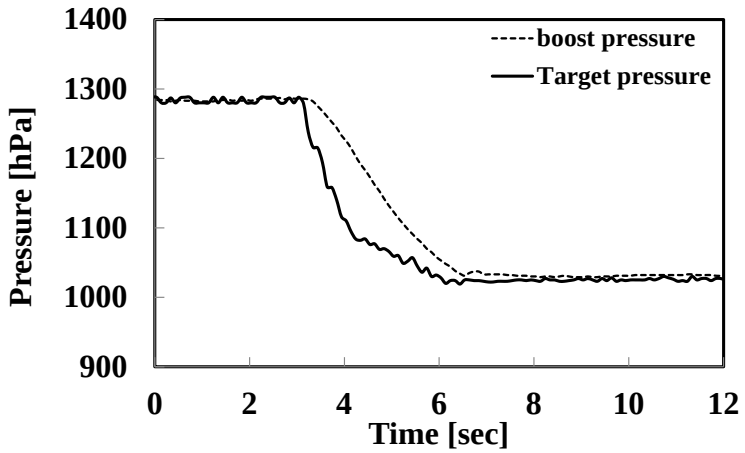

Figure 5.2 Intake manifold pressure in transient state without EGR correction logic

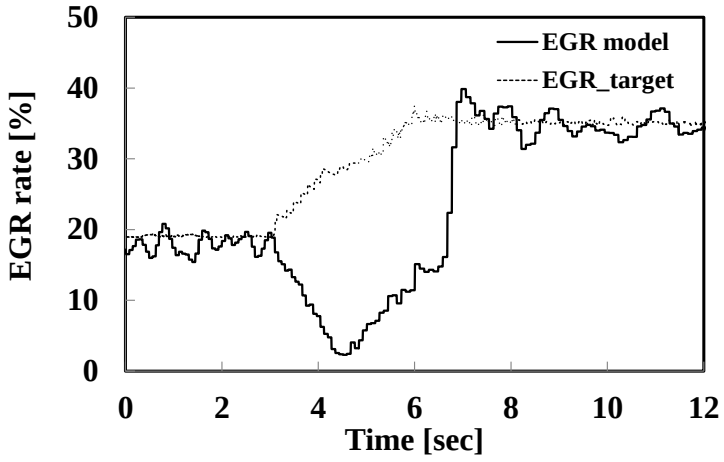

Figure 5.3 Target EGR rate and present EGR rate in transient state without EGR correction logic

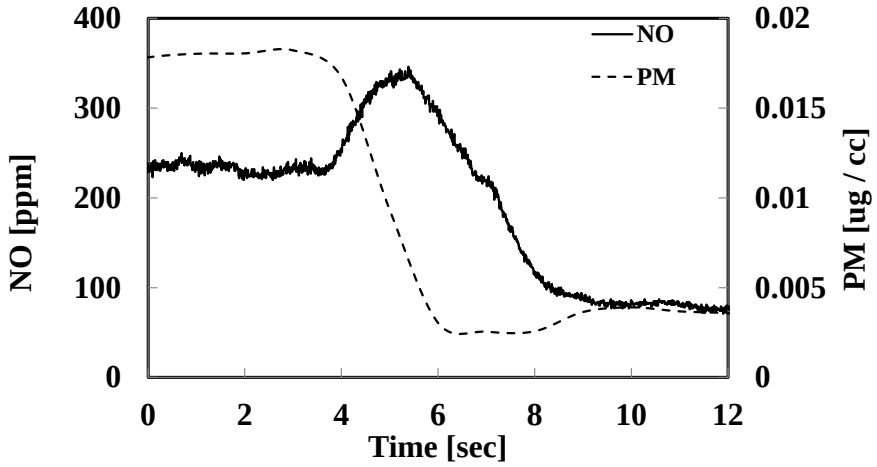

Figure 5.4 NO and PM emissions in transient state without EGR correction logic

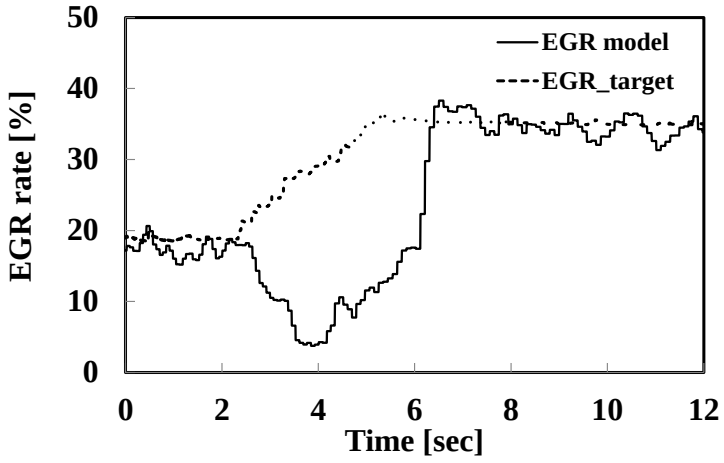

Figure 5.5 correction logic

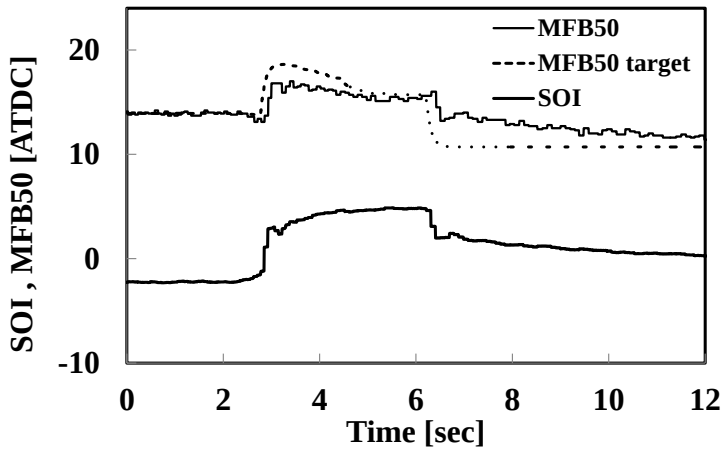

Figure 5.6 SOI, MFB50 in transient state with EGR correction logic

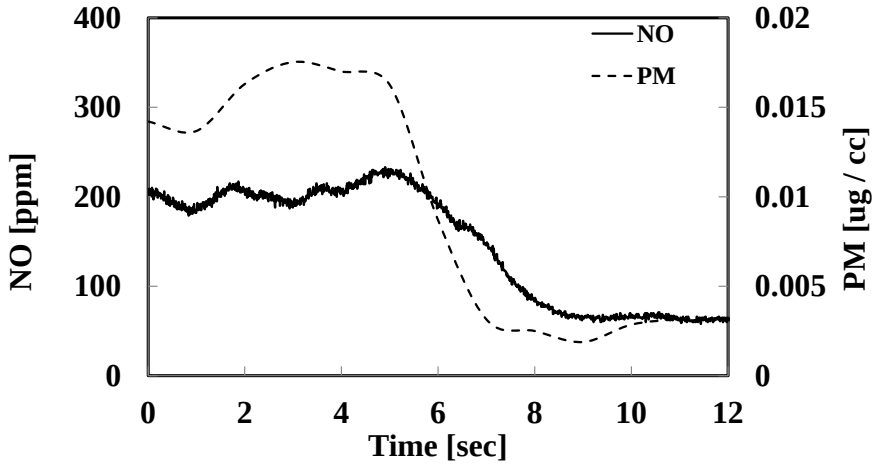

Figure 5.7 NO and PM emission in transient state with EGR correction logic

Chapter 6. Conclusions

This paper develops a model that estimated the EGR rate by measuring the temperatures of the intake manifold, the exhaust manifold and the EGR gas. Fast response thermocouples were used and heat transfer was considered to minimize the errors. The results of this model agreed well with the EGR rates measured using an exhaust gas analyzer in the steady state.

When the speed and load of the engine rapidly decreased, the EGR gas rapidly became starved in the cylinder. Thus, higher NO emissions were produced, though the load and speed were decreased. To reduce the NO emissions, an EGR correction factor is included in the closed-loop control scheme, which controls the engine based on the MFB50. The EGR rate was estimated in real-time using the EGR model with 0.1 second response time. When the difference between the target EGR rate and the estimated EGR rate exceeded a threshold, the target MFB50 was retarded so that the NO emissions were simultaneously reduced. The PM emissions were not increased during deceleration by this control scheme.

Bibliography

1. Johnson, T., "Diesel Emissions in Review," SAE Int. J. Engines 4(1):143-157, 2011, doi:10.4271/2011-01-0304.
2. Diesel Net," Cars and Light Trucks",http://www.Dieselnet.com/standards/Oct. 2012.
3. Kirchen, P.,Obrecht, P. and Boulouchos, K., "Soot Emission Measurements and Validation of a Mean Value Soot Model for Common-Rail Diesel Engines during Transient Operation", Powertrains Fuels and Lubricants Meeting (2009), 2009-01-1904, 2009, doi:10.4271/2009-01-1904.
4. HagenaJ., FilipiZ., and Assanis D., "Transient Diesel Emissions: Analysis of Engine Operation During a Tip-In", SAE world congress (2006), 2006-01-1151, 2006, doi:10.4271/2006-01-1151.
5. Kang H. and Farrell P., "Experimental Investigation of Transient Emissions (HC and NOx) in a High Speed Direct Injection (HSDI) Diesel Engine", Powertrain & Fluid Systems Conference & Exhibition (2005), 2005-01-3883, 2005, doi:10.4271/2005-01-3883.
6. Constantine D., and Evangelos G., "Diesel Engine Transient Operation",pp. 97-74, Springer, London, 2009, doi:10.1007/978-1-84882-375-4.
7. Dekker H. andSturm W., "Simulation and control of a HD Diesel engine equipped with new EGR technology", SAE paper 960871, 1996, doi:10.4271/960871.
8. MollenhauerK. And Tschoeke H., "Handbook of Diesel Engines", Springer, 2010, doi: 10.1007/978-3-540-89083-6.
9. Carlucci A., Chiara F. and Laforgia D., "Block Vibration as a Way of Monitoring the Combustion Evolution in a Direct Injection Diesel Engine", SAE paper 2006-01-1532, 2006, doi:10.4271/2006-01-1532.
10. Goldwine G., G.deBotton, Rivin B., and Sher E., "Studying the Relationship

between the Vibration Signature and the Combustion Process in Diesel Engines", SAE paper 2004-01-1786, 2004, doi:10.4271/2004-01-1786.

11. Hariyanto A., Bagiasna K., Asharimurti I., Wijaya A., Reksowardoyo K, and Arismunandar W, "Application of Wavelet Analysis to Determine the Start of Combustion of Diesel Engines", 2007-01-3556, 2007, doi:10.4271/2007-01-3556.
12. Arnone L., Boni M., Manelli S., Chiavola O., Conforto S. and Recco E.," Diesel Engine Combustion Monitoring through Block Vibration Signal Analysis", SAE paper 2009-01-0765, 2009, doi:10.4271/2009-01-0765.
13. Payri F., Broatch A., Tormos B. and Marant V., "New methodology for in-cylinder pressure analysis in direct injection diesel engines - application to combustion noise" Measurement Science Technology 16, pages 540-547, 2005, doi:10.1088/0957-0233/16/2/029.
14. Haraldsson G., Tunestal P., Johansson B. and Hyvonen J., "HCCI Combustion Phasing with Closed-Loop Combustion Control Using Variable Compression Ratio in a Multi Cylinder Engine", SAE paper 2003-01-1830, 2003, doi:10.4271/2003-01-1830.
15. Hasegawa, M., Shimasaki, Y., Yamaguchi, S. and Kobayashi, M., "Study on Ignition Timing Control for Diesel Engines Using In-Cylinder Pressure Sensor," SAE Paper 2006-01-0180, 2006, doi:10.4271/2006-01-0180.
16. Yu, S., "Study on the engine control using the in-cylinder pressure in diesel engine", Ph.D. Thesis, School of Mechanical and Aerospace Engineering, Seoul National University, Seoul, 2012.
17. Park Y., Lee H., Kim J., Lee K. and Sunwoo M., "Cylinder Air Charge Estimation for a Diesel Engine Equipped with VGT, EGR, and SCV", SAE paper 2011-01-1148, 2011, doi:10.4271/2011-01-1148.
18. Desantes J., Galindo J., Guardiola C. and Dolz V., "Air mass flow estimation in turbocharged diesel engines from in-cylinder pressure measurement", Experimental Thermal and Fluid Science 34, pages 37-47, 2010,

doi:10.1016/j.expthermflusci.2009.08.009

19. Mladek M. and Onder C. H., “A Model for the Estimation of Inducted Air Mass and the Residual Gas Fraction using Cylinder Pressure Measurements”, SAE paper 2000-01-0958, 2000, doi:10.4271/2000-01-0958.
20. Cambustion, http://www.cambustion.com/products/, Oct. 2012.
21. Han Y., Liu Z., Zhao J., Xu Y., Li J. and Li K., “EGR Response in a Turbo-charged and After-cooled DI Diesel Engine and its Effects on Smoke Opacity”, SAE paper 2008-01-1677, 2008, doi:10.4271/2008-01-1677.
22. Frank, I.,David D., Theodore B. and Adrienne L., “introduction to Heat Transfer, 5th edition, pp. 484-487,John Wiley & Sons, 2005
23. Omega, “Thermocouple Response Time”, http://www.omega.com/temperature/Z/ThermocoupleResponseTime.html, Oct. 2012.

초 록

디젤 엔진은 정상상태에 비해서 과도 상태에서 운전될 때 더 많은 유해 배출 가스를 발생한다. 이는 급기 시스템과 연료 분사 시스템간의 부조화와 터보랙 (turbo-lag) 에 의해 발생한다. 특히 급격한 과도상태에서는 터보랙으로 인해서 흡기 압력이 배기 압력에 비해 늦게 변화하게 되며 EGR의 과잉 공급이나 부족 현상을 일으킨다. 디젤엔진의 연소는 EGR 율에 민감하므로 정확한 EGR 율을 알 수 있다면 디젤 주분사시기, EGR 밸브 개도량, 연료량 등의 인자등의 제어를 통해서 배기 가스를 저감할 수 있을 것이다.

본 연구에서는 실린더로 공급되는 기체내의 EGR 율을 계산 할 수 있는 모델을 개발 하였다. 반응성이 매우 빠른 열전대를 이용하여 인터쿨러 후단의 온도, EGR 가스의 온도 및 흡기 다기관의 온도를 측정하여 에너지 보존 법칙을 이용하여 EGR 율을 계산하였다. 모델의 정확성을 높이기 위하여 흡기 다기관 내에서의 열전달을 고려하였다. 이 모델은 정상상태에서 기존의 CO_2의 농도를 통해서 EGR 율을 계산하는 기존의 방식을 통해서 검증하였다.

또한 개발된 모델을 폐회로 제어에 적용하였다. 실시간 연소 해석을 통해서 MFB50을 feedback으로 받으며 목표 MFB50을 추종하도록 주 분사

시기를 제어하도록 설계되어 있는 연소 제어기에 EGR 오차 보상 로직을 추가 하였다. 목표 EGR 율에 비해 모델로부터 계산된 현재의 EGR 율이 작을 경우 목표 MFB50을 둘의 차이에 비례하여 지각 시킴으로써 과다하게 배출 될 것으로 예상되는 NO_x를 줄 일 수 있다.

엔진의 속력과 부하가 급격히 감소하는 구간에서 실제의 EGR율이 목표 EGR 율에 비해 현저히 감소하게 되고 이에 따라 NO_x 배출이 증가 한다. 이 구간에 대하여 EGR 모델이 포함된 위의 제어 로직을 적용하였을 경우 NO_x 의 과다 발생을 억제 할 수 있음을 확인하였다.

주요어 : 직접분사식 디젤 엔진, 모델 기반 제어, 폐회로 제어, 배기가스 유해 물질, 과도 상태,

학번 : 2011-20737